

Red-Orange Emissive Cyclometalated Neutral Iridium(III) Complexes and Hydrido-iridium(III) Complex Based on 2-Phenylquinoxaline : Structure, Photophysics and Reactivity of Acetylacetonate Towards Cyclometalated Iridium Dimer

Nallathambi Sengottuvelan,^a Seong-Jae Yun,[†] Sung Kwon Kang,[‡] and Young-Inn Kim^{*}

Department of Chemistry Education and Interdisciplinary Program of Advanced Information and Display Materials, Pusan National University, Busan 609-735, Korea. *E-mail: yikim@pusan.ac.kr

[†]Department of Chemistry, Pusan National University, Busan 609-735, Korea

[‡]Department of Chemistry, Chungnam National University, Daejeon 305-764, Korea

Received March 15, 2011, Accepted October 14, 2011

A new series of heteroleptic cyclometalated iridium(III) complexes has been synthesized and characterized by absorption, emission and cyclic voltammetry studies: (pqx)₂Ir(acac) (**1**), (dmpqx)₂Ir(acac) (**2**) and (dfpqx)₂Ir(acac) (**3**) where pqx=2-phenylquinoxalinate, dmpqx=2-(2,4-dimethoxyphenyl)quinoxalinate, dfpqx=2-(2,4-difluorophenyl)quinoxalinate and acac=acetylacetonate anion. The reaction of excess acetylacetonate with μ -chloride-bridged dimeric iridium complex, [(C[^]N)₂Ir(μ -Cl)]₂, gives a complex **1** and an unusual hydrido-iridium(III) complex, (pqx)IrH(acac)₂ (**4**). The complex **1**, **2** and **3** show their emissions in an orange-red region ($\lambda_{\text{PL,max}}$ = 583-616 nm), and the emission maxima can be tuned by the change of substituent at phenyl ring of 2-phenylquinoxaline ligand. The phosphorescent line shape indicates that the emissions originate predominantly from ³MLCT states with little admixture of ligand-based ³(π - π^*) excited states. The structures of complex **3** and **4** are additionally characterized by a single crystal X-ray diffraction method. The complex **3** shows a distorted octahedral geometry around iridium(III) metal ion. A strong *trans* influence of the phenyl ring is examined. In complex **4**, there are two discrete molecules which are mirror images each other at the ratio of 1:1 in an unit cell. We propose that the phosphorescent complex **1**, **2** and **3** are possible candidates for the phosphors in OLEDs applications.

Key Words : Iridium(III) complex, Luminescence, Orange-red phosphorescence, Hydrido-iridium(III) complex

Introduction

Iridium complexes are involved in many catalytic processes such that they readily cleave hydrocarbon C-H bonds,¹ activate the OH bond in water,² dehydrogenate alkanes, alcohols, amines and ethers,³ and they are excellent candidates for optical devices due to their phosphorescent emitting phenomena.⁴ Therefore, cyclometalated iridium(III) complexes have been extensively used as active compounds in organic light-emitting diodes (OLEDs).⁵ Efficient electrophosphorescences of these iridium(III) complexes arise from the intersystem crossing from the singlet to the triplet excited state, allowing such complexes to utilize both singlet and triplet excitons. Theoretically 100% internal quantum efficiencies can be achieved for OLEDs based on phosphorescent iridium(III) complexes.⁶

Recently we reported the cationic heteroleptic iridium(III) complexes containing two 2-phenylquinoxaline-based main ligands and one ancillary imidazole ligand.⁷ The reported complexes emitted from red-orange to deep red phosphorescence with high emission quantum yields depending on the substituent of cyclometalated ligands, and we suggested them as good triplet emitters for OLEDs applications. As an

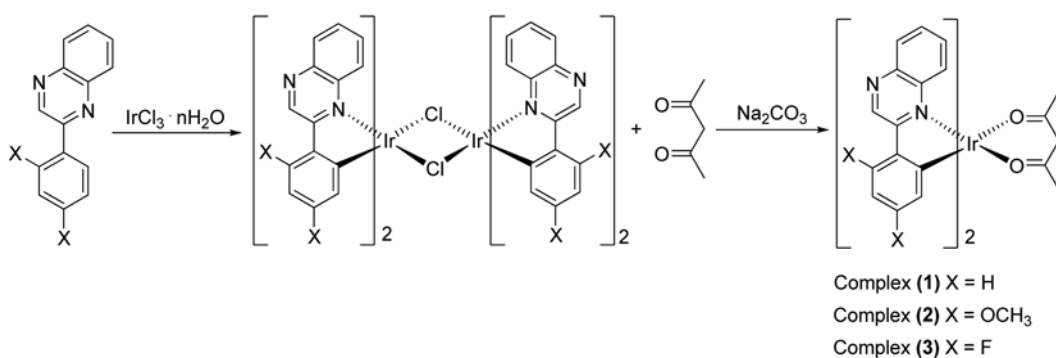
extension of our study on emissive iridium(III) complexes, herein, we synthesize cyclometalated neutral iridium(III) complexes using two 2-phenylquinoxaline-based main ligands and one acetylacetonate ancillary ligand since the nitrogen-containing heterocycles showed orange to red phosphorescent emissions⁸ and the ancillary ligand played an important role in tuning the emission color finely.^{7,9} The emissive iridium(III) complexes were prepared *via* a reaction of acac with a dimeric iridium complex [(C[^]N)₂Ir(μ -Cl)]₂ where C[^]N were 2-phenylquinoxaline-based ligands. It is worth to note that an unexpected iridium hydride complex, (pqx)IrH(acac)₂ and a luminescent (pqx)₂Ir(acac) complex were obtained when excess acac reacted with [(pqx)₂Ir(μ -Cl)]₂ dimer. This is an unusual result to afford iridium hydride compounds. A reactivity of acetylacetonate towards dimeric iridium complex is demonstrated herein. The prepared iridium(III) complexes were investigated by the structural, photophysical and electrochemical studies. We illustrate the tuning aspect of MLCT transitions to achieve a red emission.

Experimental Section

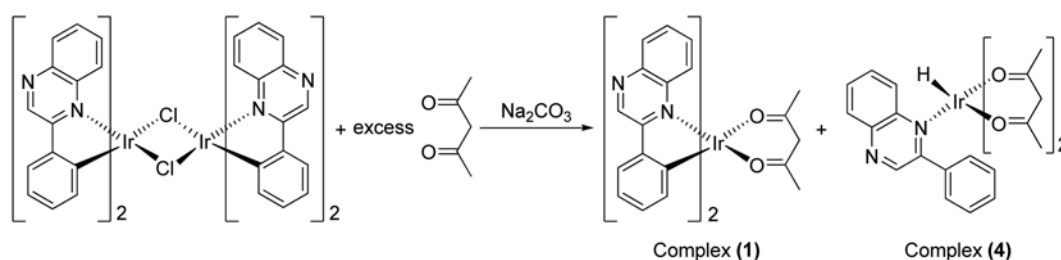
Synthesis of Iridium(III) Complexes.

Materials: All reagents and solvents were commercially obtained from Sigma-Aldrich Chemicals or Acros Organics,

^aCurrent address: Department of Chemistry, Alagappa University, Karaikudi - 630003, India



Scheme 1



Scheme 2

and used without further purification.

Synthesis of Iridium(III) Complexes. The main ligands, 2-phenylquinoxaline (pqxH), 2-(2,4-dimethoxyphenyl)quinoxaline (dmpqxH) and 2-(2,4-difluorophenyl)quinoxaline (dfpqxH) were prepared as the reported method.⁷ Cyclo-metallated iridium(III) μ -chloride-bridged dimers of general formula of $[(C^N)Ir(\mu-Cl)]_2$, where C^N represents pqx, dmpqx and dfpqx, were synthesized by a modified method reported by Nonoyama.¹⁰ The dimer complexes reacted with acetylacetonone (acacH) to afford monomeric complexes of the formula of $(pqx)_2Ir(acac)$ (1), $(dmpqx)_2Ir(acac)$ (2), $(dfpqx)_2Ir(acac)$ (3) and $(pqx)Ir(H)(acac)_2$ (4). A synthetic pathway is depicted in Scheme 1 and 2.

$(pqx)_2Ir(acac)$ (1): $[(pqx)_2Ir(\mu-Cl)]_2$ (0.50 g 0.39 mmol), sodium carbonate (0.414 g, 3.90 mmol) and 2.0 equivalent acetylacetonone (0.16 g 1.60 mmol) were dissolved in 30 mL of 2-ethoxyethanol. After degassed, the reaction vessel was maintained under nitrogen condition. Temperature was raised to 130 °C and the reaction mixture was stirred for 15 hr. The resulting dark solution was concentrated under vacuum at 60 °C and residue were eluted through a silica column to afford complex 1 as a red solid. Elementary analyses were performed at the Korean Basic Science Center. Yield: 54%. IR [cm^{-1}]: 2922, 2852, 1726, 1580, 1528, 1449, 1260. ¹H NMR (CDCl₃, 300 MHz) [ppm]: δ 1.26 (s, 6H), 4.11 (d, 1H), 6.62 (m, 2H), 6.97 (m, 2H), 7.53 (m, 2H), 7.74 (m, 2H), 8.00 (m, 2H), 8.14 (d, 2H), 8.23 (d, 2H), 8.37 (d, 1H), 8.46 (d, 1H), 9.40 (d, 1H), 9.49 (d, 1H). Anal. Calc. for C₃₃H₂₅IrN₄O₂: C, 56.48; H, 3.59; N, 7.89. Found: C, 56.56; H, 3.94; N, 7.72.

$(dmpqx)_2Ir(acac)$ (2): A similar procedure as complex 1 was followed using $[(dmpqx)_2Ir(\mu-Cl)]_2$ dimer. Dark red solid. Yield: 48%. IR [cm^{-1}]: 2925, 2853, 1580, 1739, 1580,

1483, 1397, 1268. ¹H NMR (CDCl₃, 300 MHz) [ppm]: δ 1.54 (s, 6H), 3.28 (s, 6H), 4.00 (s, 6H), 4.67 (s, 1H), 5.62 (d, 2H), 6.11 (d, 2H), 7.42 (t, 2H), 7.60 (t, 2H), 8.04 (d, 2H), 8.30 (d, 2H), 10.13 (s, 2H). Anal. Calc. for C₃₇H₃₃IrN₄O₆: C, 54.07; H, 4.05; N, 6.82. Found: C, 53.96; H, 4.95; N, 6.88.

$(dfpqx)_2Ir(acac)$ (3): A similar procedure as complex 1 was followed using $[(dfpqx)_2Ir(\mu-Cl)]_2$ dimer. Dark red solid. Yield: 42%. IR [cm^{-1}]: 2924, 2853, 2361, 1735, 1579, 1530, 1410, 1283. ¹H NMR (CDCl₃, 300 MHz) [ppm]: δ 1.58 (s, 6H), δ 4.72 (s, 1H), 5.90 (dd, 2H), 6.54 (t, 2H), 7.54 (t, 2H), 7.72 (t, 2H), 8.26(d, 2H), 8.17(d, 2H), 9.81 (s, 2H). Anal. Calc. for C₃₃H₂₁F₄IrN₄O₂: C, 51.22; H, 2.74; N, 7.24. Found: C, 51.03; H, 3.57; N, 7.15.

$(pqx)Ir(H)(acac)_2$ (4): A same procedure as complex 1 was followed using $[(pqx)_2Ir(\mu-Cl)]_2$ (0.50 g 0.39 mmol), sodium carbonate (0.414 g, 3.90 mmol) and 3.0 equivalent acetylacetonone (0.24 g 2.40 mmol) in 20 mL of 2-ethoxyethanol. The products were eluted through a silica column to afford $(pqx)Ir(H)(acac)_2$ (4) (25%) and $(pqx)_2Ir(acac)$ (1) (38%) as red solids. IR [cm^{-1}]: 2924, 2855, 2174, 1731, 1565, 1521, 1447, 1278. ¹H NMR (CDCl₃, 300 MHz) [ppm]: δ 1.82 (s, 6H), 1.92 (s, 6H), 5.20 (s, 1H), 5.50 (s, 1H), 7.56 (m, 3H), 7.75 (m, 2H), 8.12 (m, 1H), 8.19 (m, 2H), 9.00 (s, 1H), 9.53 (s, 1H). Anal. Calc. for C₂₄H₂₅IrN₂O₄: C, 48.23; H, 4.22; N, 4.69. Found: C, 49.03; H, 4.87; N, 4.15.

Physical Measurements. The IR spectra were obtained on a Perkin-Elmer FT-IR Spectrum 2000 spectrophotometer. The ¹H NMR spectra were recorded on a Varian Mercury 300 MHz instruments and chemical shifts were referenced to CDCl₃ as an internal standard. The UV-visible spectra were recorded on a Jasco V-570 UV-vis. Spectrophotometer. The photoluminescence spectra (PL) were examined at room temperature with a Hitachi F-4500 fluorescence spectro-

photometer in the range of 400–800 nm. Solution samples were degassed by three freeze pump-thaw cycles. The resulting luminescence was acquired by an intensified charge coupled detector. Electrochemical measurements were performed with a Bioanalytical Systems CV-50 W electrochemical analyzer using three electrode cell assemblies. The electrochemical cell consists of a glassy carbon working electrode, platinum wire counter electrode and Ag/AgCl reference electrode. The oxidation and reduction measurements were recorded in a dichloromethane solution containing tetra(*n*-butyl)ammonium hexafluorophosphate as a supporting electrolyte at a scan rate of 50 mV s⁻¹ under nitrogen condition. Each oxidation potential was calibrated using ferrocene as a reference. Concentration of iridium(III) complexes and supporting electrolyte were ~10⁻³ and ~10⁻¹ M, respectively.

Determination and Refinement of the X-ray Structure. X-ray intensity data were collected on a Bruker SMART APEX-II CCD diffractometer using graphite monochromated Mo K α radiation ($\lambda = 0.71073$ Å) at 174 K. Structures were solved by applying the direct method using a SHELXS-97 and refined by a full-matrix least-squares calculation on F^2 using SHELXL-97.¹¹ All non-hydrogen atoms were refined anisotropically. The hydride H atoms in complex **4**, H1 and H2, were located in a difference map and refined freely. The other hydrogen atoms were placed in ideal positions and were riding on their respective carbon atoms ($B_{\text{iso}} = 1.2 B_{\text{eq}}$ and $1.5 B_{\text{eq}}$).

Results and Discussion

Synthesis and Structural Characterization. The cyclometalated μ -chloride-bridged dimeric iridium(III) complexes, [(C^N)₂Ir(μ -Cl)]₂, are readily converted to emissive, monomeric cyclometalated complexes by treating with 2.0 equivalent of acetylacetonate in a basic condition as shown in Scheme 1: (pqx)₂Ir(acac) (**1**), (dmpqx)₂Ir(acac) (**2**) and

(dfpqx)₂Ir(acac) (**3**). It is worth to note that an unexpected mixture of products was isolated with unusual bonding patterns i.e., cyclometalated iridium(III) complex (pqx)₂Ir(acac) (**1**) and iridium(III) hydride complex (pqx)IrH(acac)₂ (**4**) when [(pqx)₂Ir(μ -Cl)]₂ was reacted with 3.0 equivalent of acetylacetonate as given in Scheme 2. These complexes were separated by a chromatographic method. The obtained (pqx)IrH(acac)₂ (**4**) complex was additionally characterized by a single crystal X-ray diffractometer. A similar reaction was reported,¹² in which the chloride-bridged dimeric iridium complex bearing the bis-sulfoxide (BTSE), [Ir₂(BTSE)₂Cl₂], reacted with 2-hydroxy-isopropylpyridine to yield the iridium(III) hydride complex, [Ir(BTSE)(2-isopropoxy-pyridine)(H)(Cl)]. The studied iridium(III) complexes are highly soluble in chlorinated solvents. IR and ¹H NMR spectral analyses are consistent with the proposed structures.

Single crystals of (dfpqx)₂Ir(acac) (**3**) and (pqx)IrH(acac)₂ (**4**) were grown by diffusion of hexane slowly into a concentrated dichloromethane solution. Their structures were unambiguously confirmed by a single crystal X-ray structure determination. Both the complex **1** and **3** crystallize in the triclinic space *P*-1. The crystallographic data and structure refinement parameters list in Table 1. The ORTEP diagrams of complex **3** and **4** are shown in Figure 1 and 2, respectively. The selected bond lengths and angles are given in Table 2. As shown in Figure 1, the iridium(III) metal ion is coordinated by three bidentate dfpqx ligands to form a distorted octahedral geometry. The *cis*-C,C and *trans*-N,N positions in the chelating dfpqx ligands were observed which is the same as in the chloride-bridged precursor complex, [(dfpqx)₂Ir(μ -Cl)]₂, indicating that the acetylacetonate ligand replaces the chloride ligand in the reaction. The bond angles around iridium(III) metal ion lie within the range of 79.78(8)–103.51(9)^o for the *cis* positioned atoms. The Ir-C bond distances (Ir-C_{av} = 1.978 Å) are shorter than those of Ir-N (Ir-N_{av} = 2.060 Å) and Ir-O (Ir-O_{av} = 2.147 Å). Ir-N bond distances are slightly longer than those of known

Table 1. Crystal data and structure refinement for complex (**3**) and (**4**)

	(dfpqx) ₂ Ir(acac) (3)	(pqx)IrH(acac) ₂ (4)
Chemical formula	C ₃₃ H ₂₁ F ₄ IrN ₄ O ₂	C ₂₄ H ₂₅ IrN ₂ O ₄
Formula weight	773.74	597.66
Temperature	174(2) K	174(2) K
Crystal system, space group	triclinic, <i>P</i> -1	triclinic, <i>P</i> -1
Space group	<i>P</i> -1	<i>P</i> -1
Wavelength (Å)	0.71073	0.71073
<i>a</i> (Å), α (°)	9.1535(18), 83.06(3)	12.5265(4), 90.144(2)
<i>b</i> (Å), β (°)	12.126(2), 77.26(3)	13.8109(5), 111.414(2)
<i>c</i> (Å), γ (°)	13.644(3), 69.04(3)	15.0374(5), 107.903(2)
Volume (Å ³)	1377.9(6)	2285.22(13)
<i>Z</i> , calculated density	2, 1.865 (Mg/m ³)	4, 1.737 (Mg/m ³)
<i>F</i> (000)	752	1168
Reflections collected/unique	27960/6849 [$R_{\text{int}} = 0.0354$]	43097/10500 [$R_{\text{int}} = 0.0408$]
Final <i>R</i> indices [$I > 2\sigma(I)$]	$R_1 = 0.0235$, $wR_2 = 0.0496$	$R_1 = 0.0357$, $wR_2 = 0.0879$
<i>R</i> indices (all data)	$R_1 = 0.0289$, $wR_2 = 0.0517$	$R_1 = 0.0539$, $wR_2 = 0.0989$
Data/Restraints/parameters	6849 / 0 / 399	10500/0/575
Goodness-of-fit on F^2	1.033	1.029

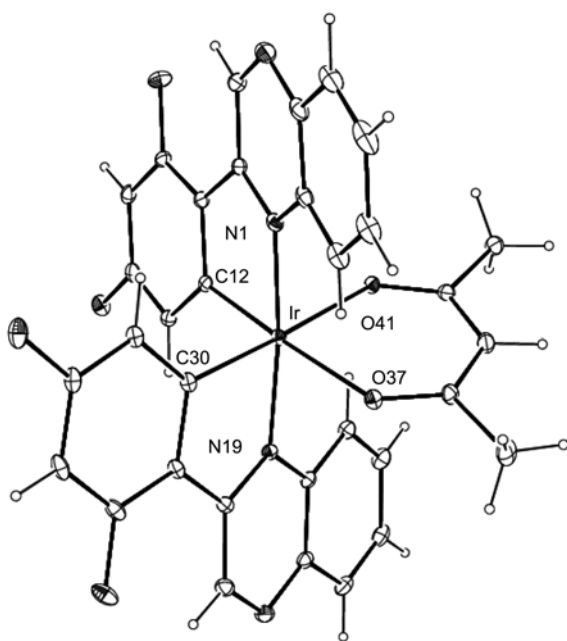


Figure 1. ORTEP diagram of complex (3), (dfpqx)₂Ir(acac), showing the atom numbering scheme with 50% probability ellipsoids.

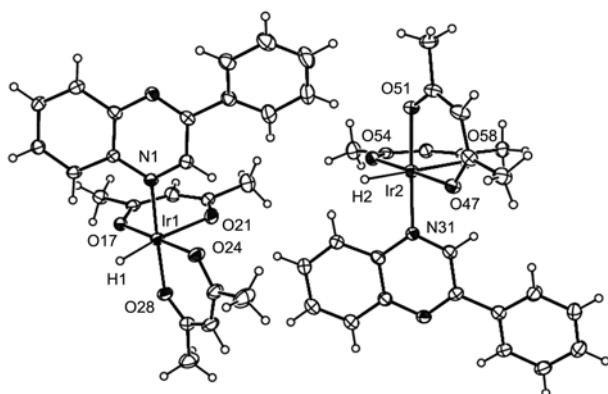


Figure 2. ORTEP diagram of complex (4), (pqx)IrH(acac)₂, showing the atom numbering scheme with 50% probability ellipsoids. Two discrete molecules are mirror images of each other.

complexes, [(tby)₂Ir(acac)]¹³ (2.040(5) Å) and [(ppy)₂Ir(acac)]¹⁴ (2.010(9) Å). The Ir-O bond distances of 2.143(2) to 2.154(2) Å are longer than the mean Ir-O value of 2.088 Å reported in the Cambridge Crystallographic Database.¹⁵ This observation can be explained by the large *trans* influence of the phenyl groups. The bite angles at iridium metal are 79.87(11) and 80.34(11)° for the cyclometalating ligands and 87.22(8)° for acetylacetonate ligand.

In the iridium hydride complex, (pqx)IrH(acac)₂ (4), there are two discrete molecules in an unit cell which are related to mirror images of each other as shown in Figure 2. These molecules exist at the ratio of 1:1 in an unit cell. The iridium(III) metal ion is six coordinated in a slightly distorted octahedral geometry defined by four acac-O atoms, one pqx-N atom and one hydride atom. Hydride H1 atom is positioned *cis* to pqx ligand. Two β-diketone acac ligands are perpendicular

Table 2. The selected bond distances (Å) and angles (°) of complex (3) and (4)

(dfpqx)₂Ir(acac) (3)			
Bond distance (Å)			
Ir-C30	1.976(3)	Ir-N19	2.071(2)
Ir-C12	1.980(3)	Ir-O41	2.143(2)
Ir-N1	2.049(2)	Ir-O37	2.154(2)
Bond angles (°)			
C30-Ir-C12	94.17(12)	N1-Ir-O41	82.60(9)
C30-Ir-N1	94.04(11)	N19-Ir-O41	103.51(9)
C12-Ir-N1	80.34(11)	C30-Ir-O37	92.84(10)
C30-Ir-N19	79.87(11)	N1-Ir-O37	102.45(9)
C12-Ir-N19	98.21(10)	N19-Ir-O37	79.78(8)
C12-Ir-O41	85.98(10)	O41-Ir-O37	87.22(8)
(pqx)IrH(acac)₂ (4)			
Bond distance (Å)			
Ir1-O17	2.017(3)	Ir1-O21	2.145(4)
Ir1-O24	2.018(4)	Ir1-N1	2.025(4)
Ir1-O28	2.021(4)	Ir1-H1	1.60(5)
Ir2-O47	2.009(4)	Ir2-O51	2.029(4)
Ir2-O54	2.025(4)	Ir2-O58	2.150(4)
Ir2-N31	2.027(4)	Ir2-H2	1.89(5)
Bond angles (°)			
O17-Ir1-O28	85.63(15)	O28-Ir1-O21	88.63(16)
O24-Ir1-O28	93.93(16)	N1-Ir1-O21	88.00(17)
O17-Ir1-N1	92.67(16)	O17-Ir1-H1	95.5(18)
O24-Ir1-N1	87.73(16)	O24-Ir1-H1	85.0(18)
O17-Ir1-O21	91.84(15)	O28-Ir1-H1	88.3(18)
O24-Ir1-O21	87.57(16)	N1-Ir1-H1	95.3(18)

to each other. The Ir-O bond distance (2.145(4) Å) *trans* to Ir-H bond is longer than those of the other Ir-O bond (2.017(3)-2.021(4) Å). The IR spectrum of (pqx)IrH(acac)₂ shows a sharp absorption at 2174 cm⁻¹ due to n(Ir-H) and a band at 1565 cm⁻¹ due to n(C=O) of the coordinated acetylacetonate ligand.¹⁶

Photophysical Properties. The UV-vis. and photoluminescence (PL) spectra of the studied iridium(III) complexes are

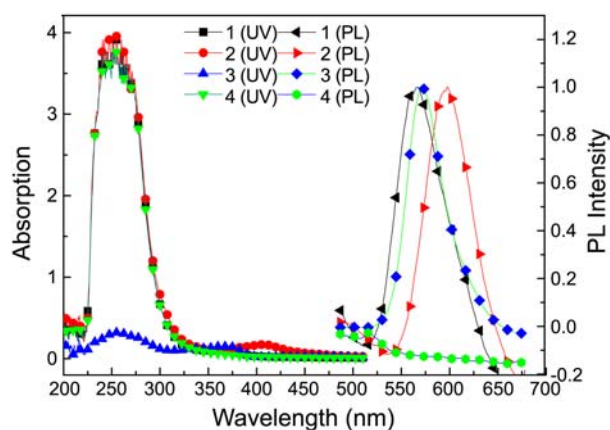


Figure 3. Absorption and emission spectra of complexes (1)-(4) in CH₂Cl₂ at room temperature.

Table 3. Photophysical and Electrochemical data of iridium(III) complexes (1)-(4)

Complex	Absorption, λ (nm) ($\epsilon \times 10^{-5} \text{ M}^{-1} \text{ cm}^{-1}$)	Emission, λ_{max} (nm)	$E_{\text{ox}}^{1/2}$ (V)	$E_{\text{red}}^{1/2}$ (V)
(pqx) ₂ Ir(acac) (1)	255 (3.45); 367 (0.09); 435 (0.02)	583	1.17	-1.27; -1.52
(dmpqx) ₂ Ir(acac) (2)	253 (3.62); 407 (0.17); 460 (0.06); 501 (0.03)	616	0.98	-1.36; -1.62
(dfpqx) ₂ Ir(acac) (3)	254 (0.32); 339 (0.13); 370 (0.15); 478 (0.03)	588	1.21	-1.68; -1.92
(pqx)IrH(acac) ₂ (4)	256 (0.36); 371 (0.05); 413 (sh)	-	1.24	-1.17; -1.50

presented in Figure 3. Table 3 lists the photophysical properties of these iridium(III) complexes. All the complexes display strong absorption bands below 253 nm which can be attributed to the π - π^* ligand-centered (LC) transitions. In addition, spin-allowed metal-to-ligand charge transfer (¹MLCT) absorption is distinguished in the region of 360 to 380 nm. On the other hand, spin-forbidden triplet ligand centered (³LC) and/or ³MLCT transitions appear as a lower energy absorption shoulder in the region of 460 to 500 nm. Strong LC and MLCT transitions were found in complex **1**, **2** and **3**.

Complex **1**, **2** and **3** exhibited spectral emissions in orange-red region. No emission peaks were observed for complex **4**. It has been reported that the phosphorescence in iridium(III) complexes comes from a mixture of ligand centered ³(π - π^*) and ³MLCT excited states depending on the energy levels of two excited states.¹⁷ The broad and featureless emissions are generally indicative that the emissions are exhibited from ³MLCT excited states whereas the vibronic fine structure with two maximum peaks arises from ³LC character.^{17,18} Complex **1**, **2** and **3** showed broad and featureless emissions, which is consistent that the emissions originate predominantly from the metal-to-ligand excited states, ³MLCT.

The emission peaks of complex **1**, **2** and **3** were examined in the range of 583 to 616 nm by varying the nature of substituent in the cyclometalated main ligand. Complex **2** bearing the electron-donating methoxy group in 2 and 4 position in the phenyl ring showed a 33 nm red shift, whereas complex **3** containing 2,4-difluorophenyl group was red shifted by 5 nm compared to complex **1**. This observation shows that the strong electron-donating group at ortho- and para- position in phenyl ring efficiently increases the HOMO energy level giving a decrease of the energy gap between HOMO and LUMO energy levels even though the exact DFT calculation is necessary for an evidence for this suggestion.

The emission wavelength can be tuned in the heterocyclic portion by a replacement one CH group by a nitrogen atom at the pyridyl fragment or further attachment of extra aromatic hexagon into a ligand framework, for example, quinoxaline ligand gives an increase of the emission wavelength compared to the hypothetical phenyl and pyrazine fragment.⁸ Therefore, the respective emission data led to the conclusion that the saturated red emission can be achieved using cyclometalated ligands containing electron-donating substituent at the phenyl group, direct nitrogen substitution for carbon at the p framework¹⁹ and extended p conjugation. For example, complex **1**, (pqx)₂Ir(acac) ($\lambda_{\text{PL,max}} = 583 \text{ nm}$) showed a red

shift compared to (ppy)₂Ir(acac)²⁰ ($\lambda_{\text{PL,max}} = 516 \text{ nm}$).

Electrochemical Studies. Complex **1**, **2** and **3** exhibited a quasi-reversible oxidation potential of 0.98 to 1.24 V and two quasi-reversible/reversible reduction processes with potential ranging from 1.25 to -1.92 V. The data are shown in Table 3. The oxidation is considered to be a metal-aryl centered process in the studied iridium(III) complexes, whereas double reversible/quasi-reversible reduction is localized mainly on the strong electron accepting heterocyclic portion of the cyclometalated ligands. The electrochemical data show that the electron-donating substituents on phenyl ring lower the $E_{\text{ox}}^{1/2}$ potential resulting in an increase of the HOMO energy level, whereas the electron-withdrawing fluorine atom increase the $E_{\text{ox}}^{1/2}$ potential. The iridium hydride complex **4** showed one irreversible oxidation at -1.24 V due to Ir^{III}/Ir^{IV} couple whereas two reversible reduction wave corresponds to the heterocyclic portion of the pqx ligand.

Conclusion

We have synthesized a series of orange-red emitting iridium(III) complex **1**, **2** and **3** bearing two 2-phenylquinoxaline(pqx)-based main ligands and one acetylacetonate ancillary ligand. We propose that complex **1**, **2** and **3** are possible candidates for the orange-red triplet emitters in OLEDs applications. Furthermore, we introduced a new iridium complex with a unique structural motif of hydrido-iridium complex (pqx)IrH(acac)₂ **4** using an excess of acetylacetonate in the reaction with the μ -chloride-bridged dimer, [(pqx)₂Ir(μ -Cl)]₂. The photophysical and electrochemical properties were discussed. The electron-donating substituent at the phenyl ring and the extended π -conjugation are effective to reduce the energy gap leading a red-shift emission. Based on phosphorescent line shape, the emissions in complex **1**, **2** and **3** originate predominantly from ³MLCT states with little admixture of ligand-based ³(π - π^*) excited states. The possible catalytic application of complex **4** and studies on electroluminescent properties of iridium(III) complex **1**, **2** and **3** are ongoing.

Supplementary Materials. Crystallographic data for the structure have been deposited with the Cambridge Crystallographic Data Center (Deposition No. CCDC-793597 and 793598). The data can be obtained free of charge via www.ccdc.cam.ac.uk/deposit (or from the CCDC, 12 Union Road, Cambridge CB2 1EZ, UK; Fax: +44-01223 336033; E-mail: deposit@ccdc.cam.ac.uk).

Acknowledgments. This work was supported by Basic Science Research Program through the National Research Foundation of Korea (NRF) funded by the Ministry of Education, Science and Technology (No. 20110003799).

References

- (a) Mkhalid, I. A. T.; Barnard, J. H.; Marder, T. B.; Murphy, J. M.; Hartwig, J. F. *Chem. Rev.* **2010**, *110*, 890. (b) Kanzelberger, M.; Singh, B.; Czerw, M.; Krogh-Jespersen, K.; Goldman, A. S. *J. Am. Chem. Soc.* **2000**, *122*, 11017.
- Morales-Morales, D.; Lee, D. W.; Wang, Z. H.; Jensen, C. M. *Organometallics* **2001**, *20*, 1144.
- (a) Jensen, C. M. *Chem. Commun.* **1999**, 2443. (b) Morales-Morales, D.; Redon, R.; Wang, Z. H.; Lee, D. W.; Yung, C.; Magnuson, K.; Jensen, C. M. *Can. J. Chem.* **2001**, *79*, 823. (c) Gu, X. Q.; Chen, W.; Morales-Morales, D.; Jensen, C. M. *J. Mol. Catal. A: Chem.* **2002**, *189*, 119. (d) Zhang, X.; Fried, A.; Knapp, S.; Goldman, A. S. *Chem. Commun.* **2003**, 16, 2060.
- Coppo, P.; Plummer, E. A.; De Cola, L. *Chem. Commun.* **2004**, 1774.
- (a) Holder, E.; Langeveld, B. M. W.; Schubert, U. S. *Adv. Mater.* **2005**, *17*, 1109. (b) Forrest, S. R.; Bradley, D. D. C.; Thompson, M. E. *Adv. Mater.* **2003**, *15*, 1043. (c) Dixon, I. M.; Collin, J. P.; Sauvage, J. P.; Flamigni, L.; Encinas, S.; Barigelletti, F. *Chem. Soc. Rev.* **2000**, *29*, 385. (d) Song, M.; Park, J. S.; Yoon, M.; Kim, A. J.; Kim, Y.-I.; Gal, Y.-S.; Lee, J. W.; Jin, S.-H. *J. Organomet. Chem.* **2011**, *696*, 2122.
- (a) Baldo, M. A.; O'Brien, D. F.; You, Y.; Shoustikov, A.; Sibley, S.; Thompson, M. E.; Forrest, S. R. *Nature* **1998**, *395*, 151. (b) Baldo, M. A.; Lamansky, S.; Burrows, P. E.; Thompson, M. E.; Forrest, S. R. *Appl. Phys. Lett.* **1999**, *75*, 4. (c) Adachi, C.; Baldo, M. A.; Thompson, M. E.; Forrest, S. R. *J. Appl. Phys.* **2001**, *90*, 5048.
- Sengottuvelan, N.; Seo, H.-J.; Kang, S. K.; Kim, Y.-I. *Bull. Korean Chem. Soc.* **2010**, *31*, 2309.
- Schneidenbach, D.; Ammermann, S.; Debeaux, M.; Freund, A.; Zöllner, M.; Daniliuc, C.; Jones, P. G.; Kowalsky, W.; Johannes, H.-H. *Inorg. Chem.* **2010**, *49*, 397.
- Ma, A.-F.; Seo, H.-J.; Jin, S.-H.; Yoon, U. C.; Hyun, M. H.; Kang, S. K.; Kim, Y.-I. *Bull. Korean Chem. Soc.* **2009**, *30*, 2754.
- Nonoyama, M. *Bull. Chem. Soc. Jpn.* **1974**, *47*, 767.
- Sheldrick G. M. *Acta Cryst.* **2008**, *A64*, 112.
- Schaul, T.; Diskin-Posner, Y.; Radius, U.; Milstein, D. *Inorg. Chem.* **2008**, *47*, 6502.
- Graces, F. O.; King, K. A.; Watts, R. J. *Inorg. Chem.* **1988**, *27*, 3464.
- Lamansky, S.; Djurovich, P.; Murphy, D.; Abdel-Razzaq, F.; Lee, H.; Adachi, C.; Burrows, P. E.; Forrest, S. R.; Thompson, M. E. *J. Am. Chem. Soc.* **2001**, *123*, 4304.
- Allen, F. H.; Davies, J. E.; Galloy, J. J.; Johnson, O.; Kennard, O.; Macrae, C. F.; Mitchell, E. M.; Mitchell, G. F.; Smith, J. M.; Watson, D. G. *J. Chem. Inf. Comput. Sci.* **1991**, *31*, 187.
- (a) Rauchfuss, T. B. *J. Am. Chem. Soc.* **1979**, *101*, 1045. (b) El Mail, R.; Garralda, M. A.; Hernández, R.; Ibarlucea, L. *J. Organomet. Chem.* **2002**, *648*, 149. (c) Garralda, M. A.; Hernández, R.; Ibarlucea, L.; Pinilla, E.; Rosario, M. *Organometallics* **2003**, *22*, 3600.
- Balton, C. B.; Murtaza, Z.; Shavez, R. J.; Rillema, D. P. *Inorg. Chem.* **1992**, *31*, 3230.
- Lamansky, S.; Djurovich, P.; Murphy, D.; Abdel-Razzaq, F.; Lee, H.-E.; Adachi, C.; Burrows, P. E.; Forrest, S. R.; Thompson, M. E. *J. Am. Chem. Soc.* **2001**, *123*, 4304.
- Ge, G.; Zhang, G.; Guo, H.; Chuai, Y.; Zou, D. *Inorg. Chim. Acta* **2009**, *362*, 2231.
- Nazeeruddin, Md. K.; Humphry-Baker, R.; Berner, D.; River, S.; Zuppiroli, L.; Graetzel, M. *J. Am. Chem. Soc.* **2003**, *125*, 8790.